preprint UMIST-TP-96/1
hep-ph/yymmxxx

Quantising the $B = 2$ and $B = 3$ Skyrmion systems

Niels R. Walet [1]

Department of Physics, UMIST, P.O. Box 88, Manchester M60 1QD, U.K.

arXiv:hep-ph/9603273v1 11 Mar 1996

Abstract

We examine the quantisation of a collective Hamiltonian for the two-baryon system derived by us in a previous paper. We show that by increasing the sophistication of the approximations we can obtain a bound state - or a resonance - not too far removed from the threshold with the quantum numbers of the deuteron. The energy of this state is shown to depend very sensitively on the parameters of the model. Subsequently we construct part of a collective Hamiltonian for the three baryon system. Large-amplitude quantum fluctuations play an important rôle in the intrinsic wave function of the ground-state, changing its symmetry from octahedral to cubic. Apart from the tetrahedron describing the minimum of the potential, we identify a "doughnut" and a "pretzel" as the most important saddle points in the potential energy surface. We show that it is likely that inclusion of fluctuations through these saddle points lead to an energy close to the triton's value.

1 Introduction

In a recent paper [1] we have investigated a numerical procedure to determine a collective coordinate manifold for the Skyrme model, and have exhibited many of the parameters in the collective Hamiltonian. At almost the same time Leese, Manton and Schroers [2] published a paper studying the quantisation of the Skyrme model in the attractive channel. Even though their collective Hamiltonian was not determined self-consistently, they obtained some very interesting results. They found a bound state at 6 MeV binding energy, with the quantum numbers of the deuteron. More importantly they found a pion density remarkably similar to that in the deuteron.

[1] electronic address: Niels.Walet@umist.ac.uk

In this paper we concentrate on a description of the deuteron using our collective Hamiltonian. We have a lot of additional information, that can be used to construct several approximations of increasing sophistication to the dynamics of the Skyrme model in the 12-dimensional manifold thought to describe the dynamics of the deuteron. We shall also exhibit the dependence on the choice of parameters in the Skyrme model, and shall argue that the result of Manton and collaborators was accidental, and that the best one can hope for is an energy not too far from zero, maybe with an error of 30 MeV or so.

After having analysed the deuteron in great detail we turn our attention to the triton and ^{3}He. A while ago, Carlson [3] has studied the application of the Skyrme model to the system of three baryons (see also Ref. [4] where the $B = 3$ system is studied using the approximate Yang-Mills instanton-induced (YMI-induced) form for the Skyrme fields). In these studies one starts from the minimum energy solution where the baryon density has tetrahedral symmetry (see Fig. 1a). One then makes the approximation that this minimum describes the triton. This approximation leads to a tremendous over-binding, which was attributed to the neglect of simple quantum effects, especially vibrational zero-point motion. It has also been mentioned [5] that anharmonic modes might play a rôle.

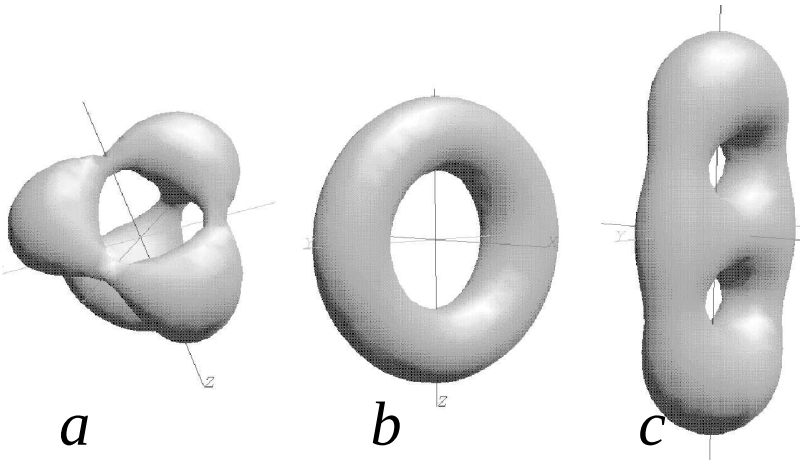

Fig. 1. A plot of a surface of constant baryon density in (a) the tetrahedron , (b) the $B = 3$ doughnut and (c) the pretzel.

In this paper we show that the low-energy potential "landscape" has a lot of structure, which has both important qualitative and quantitative effects. The most salient features in this landscape, apart from the tetrahedral solutions, are two meta-stable states at slightly higher energy, the $B = 3$ doughnut and the "pretzel" which has a planar symmetry similar to the doughnut but has two holes (see Figs. 1b and c).

The approach taken is this work is based on the techniques discussed in great detail in Ref. [1], where we show how to study large amplitude collective motion in the Skyrme model, using the YMI-induced forms of the fields for

simplicity. This is based on a mode-following approach, where we start from the harmonic fluctuations around a stable solution, and follow those into the anharmonic regime. One advantage of our approach is that such anharmonic modes always run through the extrema of the potential energy. The main limitation of the current work is the use of the instanton induced form of the Skyrme fields, see also Ref. [4].

The paper is organised as follows. In Sec. 2 we introduce the Skyrme model, and discuss the instanton-induced approximation to the dynamics of the model. We also discuss the relation of the scaled Skyrme units to standard units. We then discuss, in Sec. 3, how the study of harmonic fluctuations can be used to calculate improved observables. In the next section, Sec. 4, we succinctly recapitulate the properties of the $B = 1$ hedgehog within the YMI-induced Ansatz. We then discuss the quantisation of the $B = 2$ system in Sec. 5. In Sec. 6 we discuss the structure of the potential landscape, and how the different structures are connected. In the next section (Sec. 7) we try to estimate what the effects of the structure of the potential landscape are on the ground-state of the triton. Finally, we draw some conclusions in Sec. 8.

2 Skyrme Lagrangian, Skyrme units, and choice of parameters

2.1 The model

The "standard" Skyrme model is based on the non-linear sigma model, extended by a quartic interaction term and a pion mass term. The instanton-induced form [6,7] of the Skyrme fields can only be used in the (chiral) limit of zero pion mass, where the model is defined by the Lagrange density

$$\mathcal{L} = \frac{f_\pi^2}{4} Tr(\partial_\mu U \partial^\mu U^\dagger) + \frac{1}{32e^2} Tr[U^\dagger \partial_\mu U, U^\dagger \partial_\nu U][U^\dagger \partial^\mu U, U^\dagger \partial^\nu U], \quad (1)$$

where U is a unitary two-by-two matrix-valued field satisfying the boundary condition $U = 1$ at infinity. As has been discussed many times before, this model has a topologically conserved quantum current. The charge of this current is identified with baryon number B.

If we rescale the units of time and length, $x \to x/(ef_\pi)$, (the so-called Skyrme units), the Lagrange density takes on the slightly more convenient form

$$\mathcal{L} = \frac{f_\pi}{e} \left(\frac{1}{4} Tr(\partial_\mu U \partial^\mu U^\dagger) + \frac{1}{32} Tr[U^\dagger \partial_\mu U, U^\dagger \partial_\nu U][U^\dagger \partial^\mu U, U^\dagger \partial^\nu U] \right), \quad (2)$$

where f_π/e is the Skyrme unit of energy.

Finally the Skyrme Lagrangian can easily be reformulated in terms of the Sugawara variables (Lie-algebra valued currents) L,

$$L_\mu = U^{-1}\partial_\mu U = i\, l^a_\mu \tau_a, \tag{3}$$

and we have

$$\mathcal{L} = \frac{1}{2} l^a_\mu l^\mu_a + \frac{1}{4}\left[(l^a_\mu l^{\mu a})^2 - l^a_\mu l^a_\nu l^{\mu b} l^{\nu b}\right] \tag{4}$$

2.2 Instanton-induced Skyrme fields

As discussed in [7] one can derive a Skyrme field from a Yang Mills instanton field (called YMI-induced in this paper) by integrating the time component of the gauge potential,

$$U(\vec{x}) = C\mathcal{S}\left\{P\exp\left[\int_{-\infty}^{\infty} -A_4(\vec{x},t)dt\right]\right\}C^\dagger. \tag{5}$$

Here $\mathcal{S}$ is a constant matrix, chosen such that U decays to 1 at infinity, and C describes an overall grooming. For the current work, where we shall only consider C near the identity, it is convenient to parametrise

$$C = \exp(i\vec{\tau}\cdot\vec{\theta}). \tag{6}$$

For the Jackiw-Nohl-Rebbi (JNR) instanton of charge k we have [8]

$$A_4(\vec{x},t) = \frac{i}{2}\frac{\vec{\nabla}\rho}{\rho}\cdot\vec{\tau}, \quad \rho = \sum_{l=1}^{k+1}\frac{\lambda_l}{|x-X_l|}, \tag{7}$$

and we should use $\mathcal{S} = -I$, to obtain a field of positive baryon number k.

In order to solve for the YMI-induced value of U we convert the integral (5) to the solution of a differential equation. First introduce

$$\tilde{U}(\vec{x},\tau) = C\mathcal{S}\left\{P\exp\int_{-\infty}^{\tau} -A_4(\vec{x},t)dt\right\}C^\dagger. \tag{8}$$

This function satisfies the differential equation

$$\partial_\tau \tilde{U}(\vec{x},\tau) = -\tilde{U}(\vec{x},\tau) A_4(\vec{x},\tau), \tag{9}$$

with initial condition $U(\vec{x},-\infty) = \mathcal{S}$. The function $U(\vec{x})$ is obtained as the limit for $\tau \to \infty$ of $\tilde{U}$. We can work directly with the Sugawara variables L_μ, Eq. (3). These can be calculated as the large τ limit of a quantity $\tilde{L}_\mu$, which satisfies the differential equation

$$\partial_\tau \tilde{L}_\mu(\vec{x},\tau) = [A_4(\vec{x},\tau), \tilde{L}_\mu(\vec{x},\tau)] - \partial_\mu A_4(\vec{x},\tau). \tag{10}$$

Here the boundary condition is $\tilde{L}_\mu(\vec{x},-\infty) = 0$. By differentiating the differential equations (10) we can obtain expressions for derivatives of L_μ with respect to the instanton parameters λ_l and X_l, which will be needed later.

The field U defined in Eq. (5) does not have an explicit time dependence. There is an implicit dependence, due to a possible variation of the instanton parameters as well as the unitary matrix C (parametrised by the three angles $\vec{\theta}$) with time. Let us denote the parameters $\{\lambda_l, X_l, \vec{\theta}\}$ collectively by ξ. We then have

$$L_0 = \dot{\xi}^\alpha U^\dagger \partial_{\xi^\alpha} U \equiv \dot{\xi}^\alpha L_{,\alpha}. \tag{11}$$

If we substitute this in the Lagrangian we obtain the form

$$L = T - V, \tag{12}$$

with

$$V = \tfrac{1}{2} \sum_{i,a} l_i^a l_i^a + \tfrac{1}{4} \left[\left(\sum_{i,a} l_i^a l_i^a \right)^2 - \sum_{ij} \left(\sum_a l_i^a l_j^a \right)^2 \right], \tag{13}$$

and

$$T = \tfrac{1}{2} \dot{\xi}^\alpha \dot{B}_{\alpha\beta} \xi^\beta, \tag{14}$$

$$B_{\alpha\beta} = \sum_a l^a_{,\alpha} l^a_{,\beta} + 2 \left[\sum_a l^a_{,\alpha} l^a_{,\beta} \sum_{i,b} l_i^b l_i^b - \sum_I \left(\sum_a l_i^a l^a_{,\alpha} \sum_b l_i^b l^b_{,\beta} \right) \right]. \tag{15}$$

The Lagrangian is quadratic in the time-derivatives due to the special nature of the Skyrme model. This also means that we have broken the Lorentz invariance

of the original equations, so that (11) can only be used to describe adiabatic (small velocity) motion.

In the YMI-induced Ansatz we have thus replaced the general matrix $U(x)$, with an infinite number of parameters, by a form parametrised by $3+5(k+1)$ parameters, $CU(x|\xi)C^\dagger$.

2.3 Skyrme units and model parameters

Table 1
Different parameter sets as used in the Skyrme model

set	f_π	e
ANW	64.5 MeV	5.45
ANW′	81.7 MeV	6.95
R	90 MeV	4

We take three reasonable parameter sets in order to be able to compare the effect of changes in the parameters. The standard values for zero pion mass are those fitted by Adkins, Nappi and Witten [9] to the N and Δ masses, and are given in table 1 under the label "ANW". Since in the instanton-induced Skyrmion the moment of inertia differs considerably from its exact value, we propose a different set of parameters under the label "ANW′", that give the exact N and Δ masses for the instanton-induced fields. Finally we use a third set of parameters with realistic f_π and e. Of course we now no longer reproduce the masses.

Table 2
Our Skyrme units and their values

parameter/ units	SU	ANW	ANW'	R
[length]	$1/(f_\pi e)$	0.562 fm	0.347 fm	0.548 fm
[energy]	f_π/e	11.8 MeV	9.28 MeV	22.5 MeV
$\hbar$	e^2	29.7	48.3	16

Now it may be useful to recapitulate our units, which we have done in table 2. Note that $\hbar$ is not one in Skyrme units, but c is.

3 Harmonic expansions

In these notes we shall use a harmonic expansion around (quasi-)stable solutions of the Skyrme model. Starting from the Lagrangian (1) we can use the

instanton-induced fields to formulate a harmonic approximation of the form (we use ξ for the deviation of the coordinates from their equilibrium value)

$$H_{\rm ho} = E_0 + \tfrac{1}{2} B_{\alpha\beta}\dot{\xi}_\alpha\dot{\xi}_\beta + \tfrac{1}{2} V_{,\alpha\beta}\xi^\alpha\xi^\beta. \tag{16}$$

We can diagonalise the harmonic Hamiltonian by making a linear transformation to new coordinates (see e.g. Ref. [10])

$$\begin{aligned} q^\mu &= f^\mu_{,\alpha}\xi^\alpha, \\ \xi^\alpha &= g^\alpha_{,\mu} q^\mu, \end{aligned} \tag{17}$$

where f and g are the left and right eigenvectors of the matrix

$$M^\alpha_\beta = B^{\alpha\gamma} V_{,\gamma\beta}, \tag{18}$$

obeying the normalisation condition

$$g^\alpha_\mu f^\mu_\beta = \delta^\alpha_\beta, \tag{19}$$

and with eigenvalues $(\hbar\omega_\mu)^2$. The Hamiltonian can then be cast in the diagonal form

$$H = E_0 + {\sum_\mu}' \hbar\omega_\mu n_\mu + \sum_i \lambda_i^{-1} p_i^2, \tag{20}$$

There the first sum runs over all non-zero eigenvalues, and the second one only over the zero modes. Of course the quantised form of this same Hamiltonian can easily be obtained by replacing n_μ by $n_\mu + 1/2$, interpreting n_μ and p_i as operators. As is well known, see e.g. Ref. [11], there is a correction to E_0 (due to normal ordering of the excitation operators and the non-zero expectation value of the operators p_i in the ground state), that usually more than cancels the harmonic zero-point energy. Unfortunately, these contributions are not easily evaluated in a field theoretical context. See, however, Ref. [13].

Using similar techniques, one can easily obtain expressions for the ground state expectation values of observables. Of more direct interest when interpreting the harmonic modes is the *change* in observables related to a given mode. We shall only discuss quantities independent of the velocities. We expand

$$O = O_0 + \xi^\alpha O_{,\alpha} + \tfrac{1}{2}\xi^\alpha\xi^\beta O_{,\alpha;\beta}, \tag{21}$$

$O_{,\alpha}$ etc. are nothing more than (covariant) derivatives w.r.t. ξ^α. Of course we can apply the chain rule to convert these to derivatives w.r.t. q^μ. To linear order one finds, for small $\delta\xi$,

$$\delta O = \delta\xi^\alpha O_{,\alpha} = \delta q^\mu g^\alpha_{,\mu} O_{,\alpha}. \tag{22}$$

From which we see that

$$O_{,\mu} = g^\alpha_{,\mu} O_{,\alpha} \tag{23}$$

is a good definition of the change of O associated with the mode μ. This expression is very useful in interpretation of the harmonic modes. We can use it to define the change in baryon number, which is highly enlightening.

In order to calculate the expectation value of the operator O in the ground state we now quantise the coordinate ξ (or rather q) using the standard harmonic oscillator rules

$$\begin{aligned} q^\mu &= \left(\frac{\bar{b}^\mu}{\bar{v}^\mu}\right)^{1/4} \frac{(a^\dagger_\mu + a_\mu)}{\sqrt{2}}, \\ p_\mu &= -i\left(\frac{\bar{v}^\mu}{\bar{b}^\mu}\right)^{1/4} \frac{(a^\dagger_\mu - a_\mu)}{\sqrt{2}}, \end{aligned} \tag{24}$$

where we have used the fact that $B_{\alpha\beta}$ and $V_{\alpha\beta}$ can be diagonalised simultaneously (with eigenvalues $\bar{b}$ and $\bar{v}$, respectively). We have $\hbar\omega_\mu = (\bar{b}^\mu \bar{v}^\mu)^{1/2}$.

The quantised form of the observable O now becomes

$$\hat{O} = O_0 + \frac{1}{4}{\sum_\mu}' \left(\frac{\bar{b}^\mu}{\bar{v}^\mu}\right)^{1/2} f^\alpha_\mu f^\beta_\mu O_{,\alpha;\beta} + \text{normal ordered terms.} \tag{25}$$

The second term can now interpreted as the zero-point-motion contribution to O. Notice that everything above was done in the *intrinsic* frame (also called the body-fixed frame). In order to obtain the result for an observable in the lab frame it still has to be averaged over with a suitable rotational wave function [11].

4 Properties of the $B = 1$ hedgehog

The $B = 1$ collective Hamiltonian is given by zero-modes only,

$$H = E_0 + \frac{\hbar^2}{2\Lambda}(I^2 + S^2) + \frac{1}{2M}P^2. \tag{26}$$

The parameters in H are given in table 3, where we both show the results for the YMI-induced approximation, and for the numerical solution of the full problem.

Table 3
Properties of the $B = 1$ system.

	instanton-induced	exact
E_0	73.6 f_π/e	73.0 f_π/e
$\hbar^2/\Lambda$	1/140.1 $f_\pi e^3$	1/106.6 $f_\pi e^3$

5 Quantisation of the $B = 2$ system.

In this section we shall use the results obtained in Ref. [1] for the $B = 2$ system to make a set of approximations to the energy of the deuteron of various levels of sophistication. We shall start with a naive harmonic analysis, and end with an approximation that goes beyond the calculation by Leese *et al* [2].

5.1 Harmonic analysis.

In this section we shall discuss the harmonic analysis around the doughnut in what has been called $\mathcal{M}_{12}$ by Manton et al. This is a manifold that in the asymptotic regime has just enough collective coordinates ($12 = 6 \times 2$) to be able to project the individual Skyrmions onto nucleons. Three of those describe the centre-of-mass motion, and do not couple. The remaining 9 modes describe the intrinsic dynamics.

The issue is the understanding of bound states in this channel, where we restrict ourselves to the harmonic approximation. Since the doughnut has a continuous symmetry (generated by $M_3^{\rm int} = 2I_3^{\rm int} + J_3^{\rm int}$) we typically find two-dimensional pairs of modes when the quantum number $m_3^{\rm int}$ is changed, and 1D when it remains zero. For modes breaking the symmetry we find a centrifugal term of the form $\hbar^2/cx^2(M_3^{\rm int})^2$ (where x is a coordinate describing

the deviation from equilibrium). This leads to a 2D harmonic oscillator type spectrum, which can be given in the following form

$$E = E_0 + \sum_{2D} \hbar\omega_i (n_i + m_3^{\rm int} + 1) + \sum_{1D} \hbar\omega_i (n_i + 1/2) \\ + \frac{\hbar^2}{2\mathcal{I}_I}(I^2 - (I_3^{\rm int})^2) + \frac{\hbar^2}{2\mathcal{I}_J}(J^2 - (J_3^{\rm int})^2) + \frac{\hbar^2}{2\mathcal{I}_C}(I_3^{\rm int} - 2J_3^{\rm int})^2. \qquad (27)$$

Let me first discuss the classification of the modes:

Table 4
Harmonic frequencies around the $B = 2$ solution in the YMI-induced form.

Classification	deg.	$\lvert\Delta m_3\rvert$	$\hbar\omega\ /(f_\pi e)$
translational zero modes $(x-y)$	2	1	0
rotational zero modes $(x-y)$	2	1	0
isorotational zero modes $(x-y)$	2	1	0
translational zero mode (z)	1	0	0
mixed iso/rotational zero mode (z)	1	0	0
quadrupole mode	2	2	0.352
dipole mode	2	1	0.419
breathing mode	1	0	0.524
highest modes	2	1 (?)	0.756

Table 5
Some properties of the $B = 2$ solution in the YMI-induced form.

E_0	$141.18\ f_\pi/e$
$\hbar^2/\mathcal{I}_I$	$1/114.2\ f_\pi e^3$
$\hbar^2/\mathcal{I}_J$	$1/193.6\ f_\pi e^3$
$\hbar^2/\mathcal{I}_C$	$1/65.2\ f_\pi e^3$

We can use these number when estimating the energy in M_{12} relative to 2 $B = 1$ Skyrmions. The ground state has intrinsic quantum numbers $J = 1, I = 0, JJ_3^{\rm int} = 0, I_3^{\rm int} = 0$. We find the following energy balance:

$$\begin{array}{rrrr} & E_0 & \frac{1}{2}\sum\hbar\omega & E_{\rm rot} \\ E_{B=2} = & 141.2 f_\pi/e + & 0.771 f_\pi e + & \frac{1}{397.2} f_\pi e^3 \\ -\ 2E_{B=1} = & 147.2 f_\pi/e + & 0 \qquad\quad + & \frac{3}{2}\frac{1}{140.1} f_\pi e^3 \\ \hline \Delta E = & -6.0 f_\pi/e\ + & 0.771 f_\pi e + & -.00819\ f_\pi e^3 \end{array} \qquad (28)$$

For our three sets of parameters this takes on the values 117.7, 117.0 and 88.2 MeV.

These estimates are all unbound, but let us analyse the situation a little bit. We know first of all that the moments of inertia are usually over-estimated by the YMI-induced Skyrme-fields. Suppose we reduce all moments of inertia by a factor 106/140, corresponding to the ratio of the exact over the YMI-induced value. The ground-state energy would then decrease by 27, 57 or 15 MeV (the middle value should be disregarded, since this parameter set was already corrected for this effect).

Furthermore we have ignored the fact that we know that the behaviour in the attractive channel direction (lowest 2 modes) is a lot less harmonic than in the other direction. The difference is due to the fact that in the attractive manifold the doughnut comes apart into two hedgehogs, and the doughnut is not strongly bound. The depth of the well is 6 S.U. which takes on the values 71, 55.7 and 135 MeV for each of our three parameter sets; the harmonic energy quantum is $0.352e^2$ S.U (the e^2 is really $\hbar$ in Skyrme units), which takes values 124, 200 and 127 MeV. In the other direction we expect to reach states with energies of the order of the repulsive channel (maybe up to 1 GeV), and the harmonic approximation should be good.

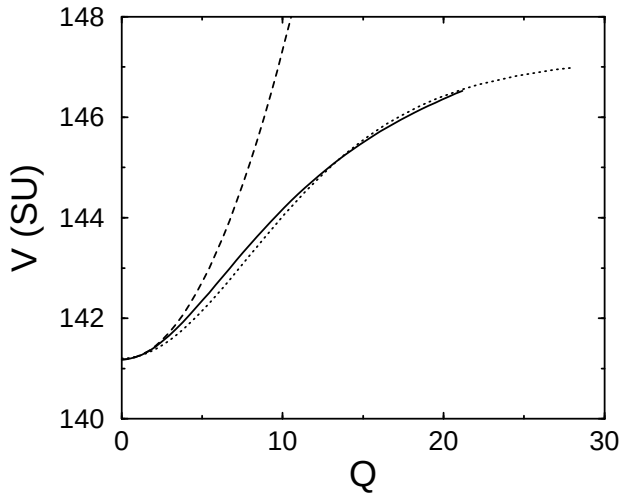

Fig. 2. The potential energy as calculated in the attractive channel (solid line). The dashed line shows the harmonic approximation to this potential, and the dotted line a Pöschl-Teller fit

In order to see what might be the possible effect of the limited well-depth we also calculate the binding energy of the lowest state by approximating the potential by a Pöschl-Teller form [14]. This has the advantage that the problem is exactly soluble, and this potential has only two parameters, which can be chosen to be the depth and the harmonic frequency. If more information is known one of the generalised potentials discussed by Ginocchio [15] might be

of some use. For the time being we use the form

$$V(x) = -\nu(\nu+1)/\cosh^2(\alpha x). \tag{29}$$

Here we have chosen our coordinates such that $\hbar^2/m = 1$. The parameters ν and α can then be connected to the harmonic frequency and the depth of the potential

$$\begin{aligned} \nu &= \frac{1}{2}(-1+\sqrt{1+8V_0/\alpha^2}), \\ \alpha &= \hbar\omega/\sqrt{V_0}. \end{aligned} \tag{30}$$

For this exactly solvable potential we then find that the ground state occurs at a zero-point energy

$$E_0 = \frac{\hbar\omega}{2}\left[\frac{\hbar\omega}{4V_0}\left(\sqrt{1+16\left(V_0/\hbar\omega\right)^2}-1\right)\right] \tag{31}$$

above the minimum of the potential. It is easy to see that this reduces to the harmonic oscillator value in the limit $V_0 \gg \hbar\omega$.

The reduction in the contribution for our lowest two modes would be 0.655, 0.518 and 0.768 for our three parameter sets. This corresponds to 43, 96 and 30 MeV reduction in binding. Taking all corrections together (we do not correct the middle value for the wrong value of the moment of inertia) we find 47, 21 and 43 MeV. These values are reasonably close to zero, which is about the best one could hope for such a crude calculation. We have summarised our calculations in table 6.

Table 6
Summary of harmonic and related approximations for the deuteron energy relative to the $B = 2$ threshold, as discussed in the text.

	ANW	ANW′	R
harmonic	118 MeV	117 MeV	88 MeV
corrected moment of inertia	98 MeV	117 MeV	73 MeV
include anharmonicity	47 MeV	21 MeV	43 MeV

5.2 Quantisation in M_7 and extensions

Leese, Manton and Schroers have constructed a Hamiltonian in the attractive channel, where one has 7 degrees of freedom. A quantisation of this Hamilto-

nian in the intrinsic frame led to a binding energy of 6 MeV. From our calculation a similar Hamiltonian is available, and it would be nice to independently check these predictions, and we have all the necessary ingredients. [2] We normalise our collective coordinate such that the mass is 1 in Skyrme units, and we then have to quantise the intrinsic collective Hamiltonian (see also Ref. [2])

$$H = \tfrac{1}{2}\left(P^2 + \frac{(J_x^{\rm int})^2}{a(Q)^2} + \frac{(J_y^{\rm int})^2}{b(Q)^2} + \frac{\left[J_z^{\rm int} - w(Q) I_z^{\rm int}\right]^2}{c(Q)^2} + \frac{(I_x^{\rm int})^2}{A(Q)^2} + \frac{(I_y^{\rm int})^2}{B(Q)^2} + \frac{(I_z^{\rm int})^2}{C(Q)^2} \right) + V(Q). \tag{32}$$

Using the standard geometrical quantisation, and the intrinsic quantum numbers compatible with the deuteron, $I = 0, J = 1, J_z^{\rm int} = 0$, we obtain a "radial" equation of the form

$$\left[-\tfrac{1}{2} \frac{\hbar^2}{g^{1/2}} \partial_Q \left(g^{1/2} \partial_Q \right) + \hbar^2 \left(\frac{1}{2a^2} + \frac{1}{2b^2} \right) + V(Q) \right] \psi(Q) = E \psi(Q). \tag{33}$$

Here $g^{1/2}$ is the square-root of the determinant of the metric (mass matrix),

$$g^{1/2} = abcABC. \tag{34}$$

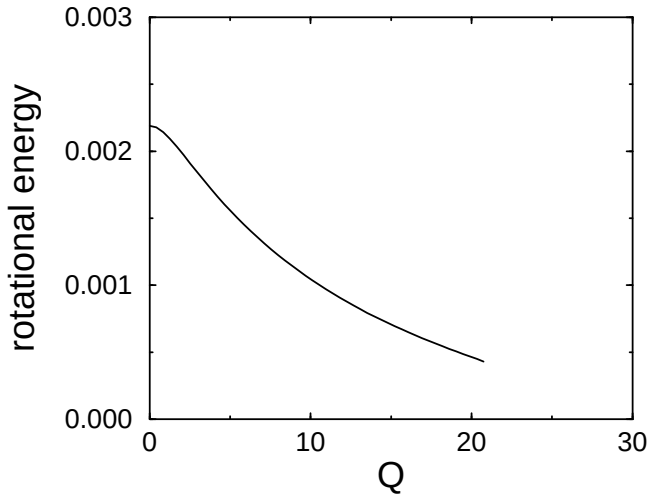

Fig. 3. The contribution of the rotational kinetic energy to the deuteron bound-state problem.

[2] Note that there is an error in the collective coordinate Q as presented in Ref. [1], as well as a factor of two difference in the inertial parameters. The results presented here use the corrected Q.

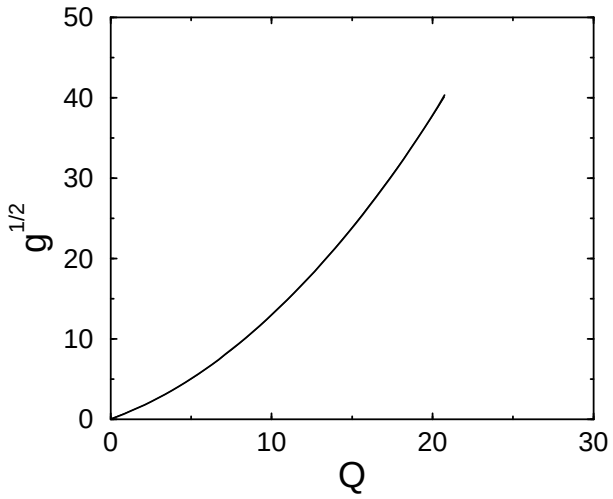

Fig. 4. The metric factor $g^{1/2}$ in the kinetic energy, rescaled by a constant.

The contribution of the rotational kinetic energy, which has units $f_\pi e^3$, is plotted in Fig. 3. We have subtracted the asymptotic behaviour – which corresponds to the system separating into two hedgehogs locked in the attractive configuration. This is not the same as subtracting the kinetic energy of two hedgehogs in nucleon states. This would require that one includes the harmonic motion changing to zero-mode motion as the hedgehogs pull apart. This can (and should) only be done for scattering states [16]. For a bound-state calculations this part is missing (see below), one should only subtract so much rotational zero-point energy as to put the ionisation barrier at 0.

The metric factor $g^{1/2}$ (scaled by a constant) is plotted in Fig. 4. It is very well fitted by a form $\alpha Q + \beta Q^2$. The proportionality to Q for small Q agrees with the two-dimensional harmonic nature of the motion there. The asymptotic behaviour agrees with the result by Leese *et al.* Mathematically one can interpret this as a system that changes it nature from two-dimensional at small Q to 3D at large separations. We have fitted all the relevant quantities as a function of separation, taking into account the exact behaviour for large separation. This allows one to solve the Schrödinger equation numerically. Some selected results are presented in table 7.

In order to mimic the effects of quantising in the full 12-dimensional configuration space corresponding to full translational and iso-rotational zero modes of the two hedgehogs that appear at large separation we add the harmonic zero-point energies for these modes. Let us first study a correlation diagram, that shows all the non-zero modes as they develop from the doughnut, see Fig. 5. As one can see over there counting modes causes some problems. The lowest two modes correspond to the attractive channel, and the next two modes are the ones describing the two remaining fluctuations in M_{12}. The problem lies in the level crossing at $Q = 8.8$. If this were an avoided crossing, we would

Table 7
The energy of the lowest bound state in units of f_π/e as a function of e. The three columns denote the pure potential (no rotational energy), potential plus rotational energy and the additional effect of also adding the harmonic zero-point energies for the other modes in M_{12}. A dash indicates no solution.

e	potential	rotational	all
1	-5.67	-5.67	-5.49
2	-4.94	-4.63	-4.43
3	-3.95	-3.83	-2.47
4	-2.67	-2.32	-0.30
5	-1.28	-0.65	—
6	-.0044	—	—

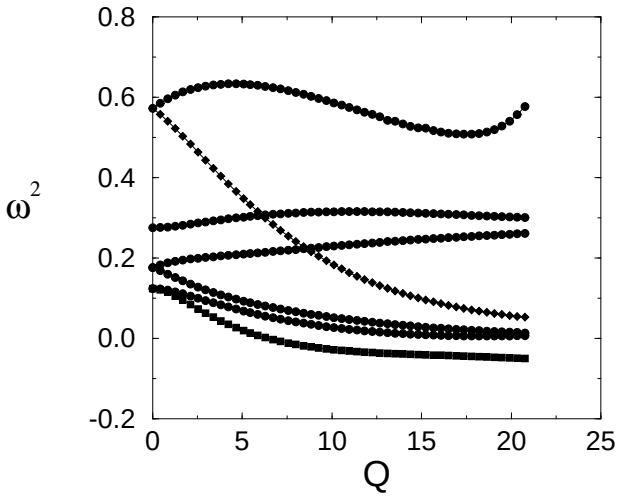

Fig. 5. A correlation diagram, showing how the local harmonic frequencies are correlated as we move from the doughnut in the attractive channel.

happily follow the lowest mode. Unfortunately it is not: there is quite a lot of symmetry in the attractive channel and the two modes appear to have *different* symmetries. This may be an artifact of the YMI-induced Ansatz, but it seems more likely that this is a real effect. Since this symmetry is closely linked to the attractive channel, it is highly probable that if we deform the system a little bit away from the attractive channel, we get an avoided crossing. The crossing point would then correspond to what has been termed a diabolic point in the theory of Berry's phases, and lead to a monopole type geometric phase. For the time being we ignore this effect and shall sum the zero-point energy of the two lowest modes, as shown in Fig. 6.

Results including this harmonic contribution are give in the third column of table 7. Taking all the results together, we are forced to conclude that

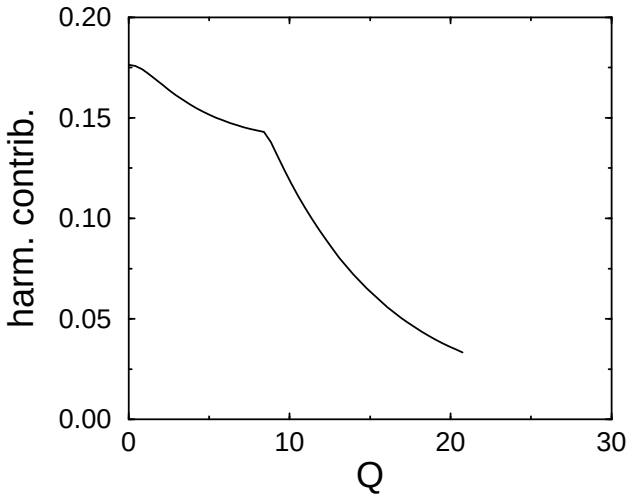

Fig. 6. The harmonic energy as added to the collective Hamiltonian.

is almost impossible to find a bound state for a reasonable set of parameters when disregarding the harmonic motion, whereas when including the harmonic motion a value for e of at most four is allowed. This is a contradiction of the claim of 6 MeV binding energy by Leese *et al* [2]. They used a set of Skyrme parameters appropriate to a finite pion mass, however, without examining the parameter dependence. The fact that there is a bound state close to zero energy, or a resonance slightly above is the most important issue. One cannot consider the model to be right on scales of the order of a few MeV out of 2GeV, especially not without including loops and the related counterterms [13].

6 The structure of the $B = 3$ collective manifold

6.1 Harmonic modes around the tetrahedron

For the $B = 3$ case we use the YMI-induced+JNR form as used by Leese and Manton [4]. This is not based on the most general instanton field but is probably sufficiently general for our purposes.

The instanton field is generated by four poles, arranged in an tetrahedron. All weights are equal. We choose

$$(\lambda_1, X_1) = (1/4, -R, -R, -R, 0),$$
$$(\lambda_2, X_2) = (1/4, -R, R, R, 0),$$
$$(\lambda_3, X_3) = (1/4, R, -R, R, 0),$$

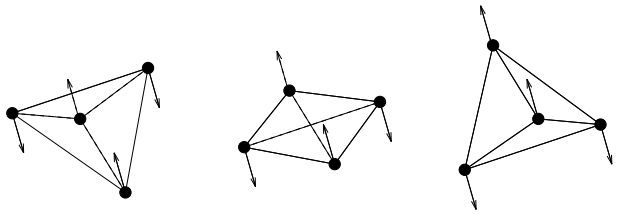

Fig. 7. Tunnelling from one tetrahedron to another.

$$(\lambda_4, X_4) = (1/4, R, R, -R, 0), \tag{35}$$

where R is a parameter determining the size of the tetrahedron.

Since all continuous symmetries are broken, we find 9 zero modes. The remaining modes can be classified as follows (The interpretation and classification of these modes is discussed in more detail in the appendix):

10-11 $\hbar\omega = 0.318 f_\pi e$.
These two modes correspond to the motion towards the $B = 3$ doughnut, See Fig. 7 for a sketch.

12-14 $\hbar\omega = 0.332 f_\pi e$.
These modes are the beginning of a trajectory towards the pretzel mentioned in the introduction.

15-17 $\hbar\omega = 0.469 f_\pi e$.
It is highly probable that these modes describe the separation in a $B = 2$ doughnut and a single hedgehog.

18 $\hbar\omega = 0.483 f_\pi e$.
This is the breathing mode.

19-21 $\hbar\omega = 0.813 f_\pi e$. These are the only modes that mix with iso-spin rotations. They describe a complex high-energy excitation.

If we assume that we need 18 modes to describe the $B = 3$ collective coordinates, we notice that there is a clear gap in the spectrum just at that critical point. We have not used the most general instantons here, and it is unlikely but not impossible that this situation might change if we switch to the AHDM instanton [21].

Table 8
Some properties of the $B = 3$ solution in the YMI-induced form.

E_0	$206.6\ f_\pi/e$
$\hbar^2/\mathcal{I}_I$	$(113)^{-1}\ f_\pi e^3$
$\hbar^2/\mathcal{I}_J$	$(357)^{-1}\ f_\pi e^3$
$\hbar^2/\mathcal{I}_C$	$(-633)^{-1}\ f_\pi e^3$

As said before, the lowest non-zero modes of the tetrahedron correspond to motion towards the $B = 3$ doughnut, where the line connecting any of the corners of the tetrahedron moves closer to the line connecting the other two

corners. When these lines cross we have reached the $B = 3$ doughnut which in our Ansatz is described by four poles arranged in a square. Actually one would expect three such modes, one for each coordinate axis. However, the sum of these modes is the breathing mode, which is in a different representation of the tetrahedral group, and thus we find only two modes (see also our model discussion below). Following these modes naturally leads one to study the doughnut as well. It sits on the top of a saddle-point in energy. It has two unstable modes, whereas we expected only one corresponding to the path towards the tetrahedron. Indeed this is the most unstable mode. The other unstable mode leads to yet another saddle point. This solution has the double-hole structure of a pretzel. The potential energy of all these states, *i.e.*, ignoring contributions from the rotational kinetic energy, is not very different

$$E_{\rm tetrahedron} = 206.56 f_\pi/e, \quad E_{\rm pretzel} = 211.54 f_\pi/e, \quad E_{\rm doughnut} = 214.06 f_\pi/e,$$
$$3E_{B=1} = 220.8 f_\pi/e, E_{B=2} + E_{B=1} = 214.8 f_\pi/e. \tag{36}$$

As one can see from table 9 the sizes of the different configurations are different. Here we have given the values of the integrals

$$\langle r_i^2 \rangle = \int r_i^2 B(\vec{r}) d^3 r, \tag{37}$$

which is the standard definition for these quantities.

Table 9
Sizes of the different shapes for $B = 3$ in S.U.

solution	$\langle xx \rangle$	$\langle yy \rangle$	$\langle zz \rangle$	$\langle r^2 \rangle$
tetrahedron	3.043	3.043	3.043	9.129
pretzel	9.225	2.436	.916	12.577
doughnut	4.974	4.974	.878	10.836

Let us first consider the paths connecting the different solutions. As we stated there is a path connecting the two independent tetrahedral configurations through a saddle point that looks like a doughnut. Actually there are three such paths, corresponding to the three "independent" doughnuts with rotational symmetry around each of the three coordinate axes. Such a path is very similar to the geodesic with twisted symmetry found in the scattering of three collinear monopoles by Houghton and Sutcliffe [17]. It corresponds to motion where the Skyrmion breaks apart into three $B = 1$ hedgehogs in an attractive (and therefore twisted) configuration. The only thing is that in our case the Skyrmion does not go into into this form, but rather breaks up into two $B = 3/2$ "bananas" as shown in Fig. 8. Since solutions with fractional baryon number do not exist in the Skyrme model – they have infinite energy – this

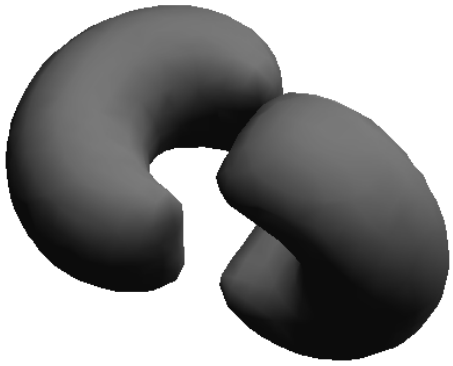

Fig. 8. An example of the baryon density found when following the path through the doughnut and the tetrahedron, to a point beyond the tetrahedron

leads to an infinite energy in the limit of infinite separation. It is plausible that the use of the JNR instanton, instead of the full AHDM data is responsible for this effect – It is hard to imagine how to describe the desired configuration in terms of the JNR data. For the motion *in between* the doughnut and hedgehog the JNR form appears to be reasonable.

In Fig. 9 we show how the local harmonic frequencies change as we move from the doughnut to the tetrahedron and beyond. As usual we have fixed the normalisation of the coordinate Q by requiring that the mass (which we usually call $\bar{B}$) equals one. There are no major exciting structures along the path, and one can see that the mode we followed (denoted by the triangles) interpolates smoothly between the tetrahedron and doughnut. Furthermore we find that several modes are doubly degenerate for all Q due to the symmetry in the configurations along the path. In this case ignoring the weights in the JNR instanton is no limitation; they are constant and all equal for all points along the path. The potential energy along the path is given in Fig. 10.

Once one has the doughnut, one can study its unstable modes. It has two, the one discussed above, and one leading to the pretzel. This latter solution is described by a rhombic arrangement of the poles, so that for each doughnut we have two neighbouring pretzels, obtained by compressing any of the two diagonals of the square arrangements of poles describing the doughnut. In this case the weights in the JNR potential are also no longer equal, but this need not concern us here. The pretzel has one unstable mode, which connects to the tetrahedron, as we discovered through our mode following approach.

A very important property of the path between the tetrahedron and the pretzel is that at all points the Skyrme fields have a trivial reflection symmetry under coordinate reflections, namely $\vec{\phi}(R_i\vec{x}) = R_i\vec{\phi}(\vec{x})$.

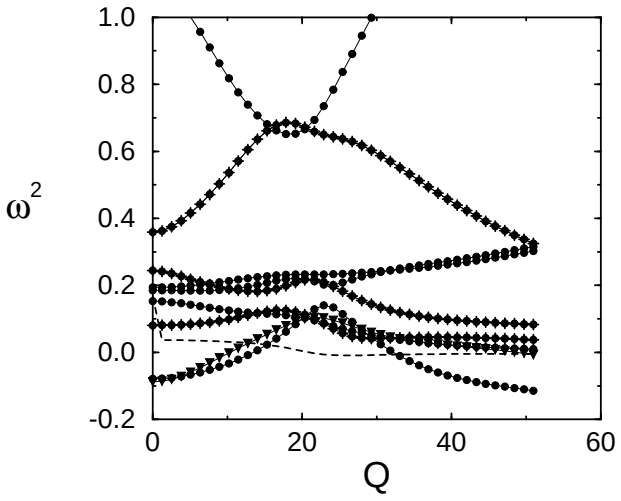

Fig. 9. A correlation diagram, showing how the local harmonic frequencies are correlated as we move from the doughnut to the tetrahedron (at $Q \approx 20$) and beyond. The lines with pluses and circles are doubly degenerate. The triangles are used to label the mode actually followed. The dashed line shows the new (zero-)mode appearing when we move away from the doughnut. Note that this connects to a non-zero mode at the doughnut. This is probably another deficiency of the JNR parametrisation.

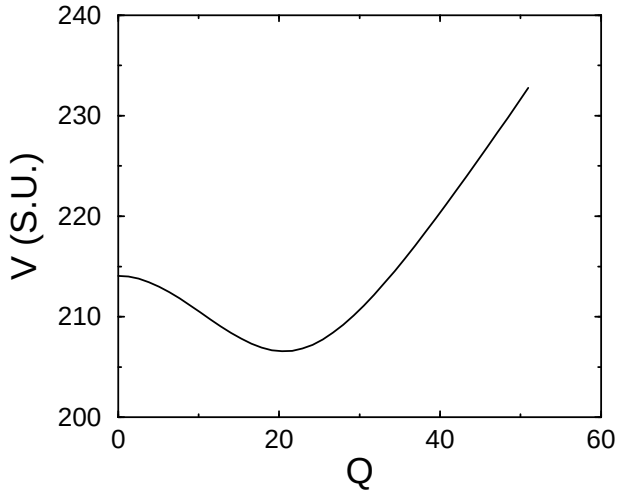

Fig. 10. The potential energy as a function of the coordinate Q, as we move from the doughnut to the tetrahedron (at $Q \approx 20$) and beyond. Note the steep rise of the potential, above the "ionisation" limit of 220.8 S.U., when the system splits into two $B = 3/2$ "bananas".

In Fig. 11 we show how the local harmonic frequencies change as we move from the pretzel to the tetrahedron. Actually we find that at the tetrahedron the mode followed (again denoted by squares) connects to the lowest triplet of modes in the doughnut. Since each of the modes of the triplet describes a

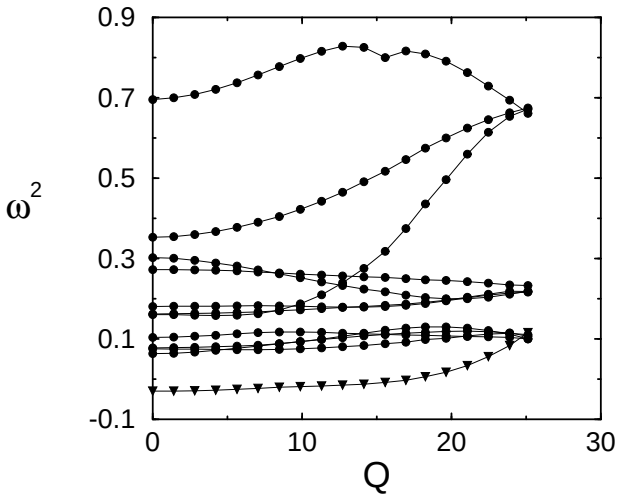

Fig. 11. A correlation diagram, showing how the local harmonic frequencies are correlated as we move from the pretzel ($Q = 0$) to the tetrahedron (at $Q \approx 25$).

circuit through two pretzels and another tetrahedron, as denoted schematically in Fig. 12. Note that the lowest mode for the tetrahedron is the one connecting

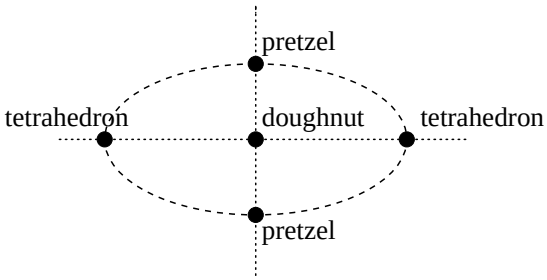

Fig. 12. A schematic sketch of a few of the connections through a given doughnut. For each doughnut in one of the three coordinate planes, there are two associated pretzels, elongated along one of the two coordinate axes in the plane, and connected by a valley. There is a connection of the doughnut to two tetrahedra with different orientations. There also exists a closed valley connecting the tetrahedra through the pretzels.

to the doughnut, which is the higher of the two saddle points. Obviously this figure only sketches one out of three connections, the whole structure of the collective manifold being highly complex.

7 Quantisation of the collective coordinates

7.1 Harmonic approximation

As in the case of the $B = 2$ system, the most straightforward way to get a "quantum" result for $B = 3$ is to quantise in harmonic approximation. Near the tetrahedron the collective Hamiltonian leads to an expression for the energy of the following form

$$\begin{aligned} E = E_0 + \sum_{\text{modes}} \hbar\omega_i (n_i + 1/2) \\ + \frac{\hbar^2}{2\mathcal{I}_I} I^2 + \frac{\hbar^2}{2\mathcal{I}_J} J^2 + \frac{\hbar^2}{2\mathcal{I}_C} \vec{I} \cdot \vec{J}. \end{aligned} \tag{38}$$

The ground state has intrinsic quantum numbers $I = 1/2, J = 1/2, K = 0$. Replacing the inner product of I and J with the square of the grand-spin operator K, we find the following energy balance:

$$\begin{array}{rrrr} & E_0 & \frac{1}{2}\sum\hbar\omega & E_{\text{rot}} \\ E_{B=3} = & 206.6 f_\pi/e & + 1.76 f_\pi e & + .00353 f_\pi e^3 \\ -\ 3E_{B+1} = & 220.8 f_\pi/e & + 0 & + \frac{9}{4}\frac{1}{140.1} f_\pi e^3 \\ \hline \Delta E = & -14.2 f_\pi/e & + 1.76 f_\pi e & - 0.0125 f_\pi e^3 \end{array} \tag{39}$$

For our three sets of parameters this takes on the values 319.2, 386.5 and 242.1 MeV. Here we once again see the effect of the over-estimate of quantum corrections. Notice that without these corrections the value would be -168, -132 and -320 MeV, respectively. Since we expect anharmonicities to play a large rôle, we shall now study the effect of large amplitude fluctuations.

7.2 Approximate large-amplitude dynamics

As a fast and relatively simple way to study the modes one can assume that one can independently quantise the motion along the straight line and the ellipse, since these represent orthogonal modes at the tetrahedron.

We first look at the paths through the doughnut. We have constructed a simple model, based on the VSEPR model [12], as has been used in the chemistry of molecules. It is based on putting particles on a sphere, and letting them interact through a pairwise repulsive interaction, which is taken to be some power of the inverse of the separation of the particles. If we do that in our problem we should constrain the JNR poles on a sphere. The minimal energy

configuration will be a tetrahedron, and there will be a saddle point at the a square configuration of poles, corresponding to the doughnut. The configuration space is an eight-dimensional manifold. Three of those are the rotational zero modes. At the tetrahedron the remaining modes are a pair of degenerate modes describing the motion towards the squares and three further-non-zero modes. These last three are of no interest, but can be eliminated by imposing the additional constraint that the distance between two pairs of points is equal, and that the line connecting the two mid-points of each pair goes through the centre of the sphere.

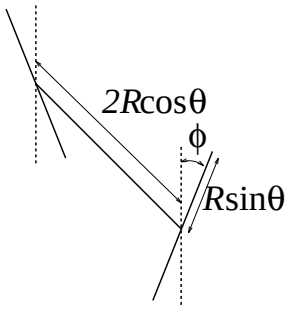

Fig. 13. Coordinates used in our VPSER-based model.

With these constraints, using the coordinates specified in Fig. 13, we obtain

$$\vec{r}_1 = RD(\Omega)(\sin\theta\cos\phi, \sin\theta\sin\phi, \cos\theta), \tag{40}$$
$$\vec{r}_2 = RD(\Omega)(-\sin\theta\cos\phi, -\sin\theta\sin\phi, \cos\theta), \tag{41}$$
$$\vec{r}_3 = RD(\Omega)(\sin\theta\cos\phi, -\sin\theta\sin\phi, -\cos\theta), \tag{42}$$
$$\vec{r}_4 = RD(\Omega)(-\sin\theta\cos\phi, \sin\theta\sin\phi, -\cos\theta). \tag{43}$$

(Here $D(\Omega)$ is a rigid body-rotation corresponding to the three zero-modes). From this we can calculate the classical Lagrangian,

$$\begin{aligned}\mathcal{L} &= \tfrac{1}{2}\sum_i \dot{\vec{r}}_i^2 - \sum_{i<j} 1/|r_i - r_j|^{2n} \\ &= 2R^2(\dot{\Omega}^2 + \dot{\theta}^2 + \sin^2\theta\dot{\phi}^2) \\ &\quad -2/4^n\left(1/(\sin^2\theta)^n + 1/(\cos^2\theta + \sin^2\theta\sin^2\phi)^n + \right. \\ &\quad \left. 1/(\cos^2\theta + \sin^2\theta\cos^2\phi)^n\right). \end{aligned} \tag{44}$$

A lot of insight can be gained by plotting the potential as a function of θ and ϕ. The kinetic energy is proportional to $\vec{L}^2$, which allows the interpretation of the configuration space as a sphere. In order to plot the potential on this sphere, we have colour-coded the values of V. In Fig. 14 one can see this potential. We have also indicated the tunnelling paths from one minimum to the next. Here one can see why we have only two independent modes, and not three: one can not have three *orthogonal* paths in two dimensions.

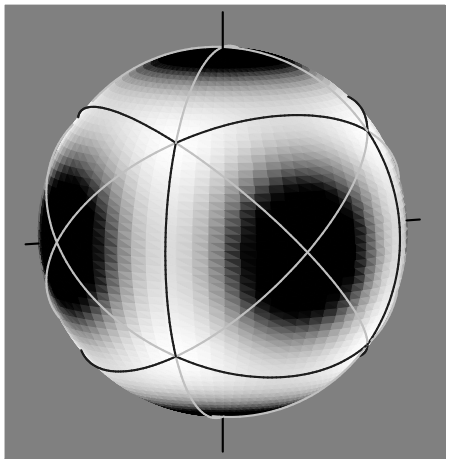

Fig. 14. The potential energy (44) plotted as a function of θ and ϕ. The white areas denote lowest potential energy, the black areas are where the potential diverges. The black lines show the tunnelling paths between different minima; the gray lines are the continuation of the black ones into the repulsive regime.

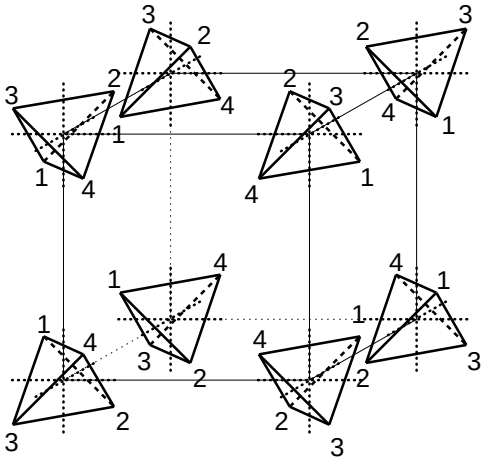

Fig. 15. Orientation of the tetrahedra corresponding to each of the vertices of the cube in Fig. 16

One has to be somewhat careful how to interpret this sphere. In essence there are only two independent orientations of the tetrahedron (the minimum), which are related through an element of the octahedral group that is not in the tetrahedral group. A sketch of that is given if Fig. 15. As can be seen there, adjacent vertices have independent tetrahedra, whereas all next-to-nearest neighbours correspond to the same tetrahedron and a relabelling of the poles. This relabelling does nothing for the Skyrme fields, and we are thus forced to identify these configurations as the same point. This tetrahedral invariance means that the quantum mechanics is actually restricted to a quarter of the sphere, with slightly complex boundary conditions. The potential energy has an even higher symmetry, however. Its fundamental domain, 1/24th of the sphere, is mapped onto the whole sphere by the O_h group. Qualitatively one would expect that the lowest state has maximal symmetry. This is realized

if we make a symmetric combination of individual wave functions located in each minimum, leading to a cubic arrangement of wave functions. Note that this is not directly related to the pole positions; each minimum corresponds to a different tetrahedron. They can be arranged in two groups of four. Within each group the tetrahedra are related by a permutation of the poles (or an element of the tetrahedral group). The two groups are related by a 90° rotation, an element of the octahedral group. Since the pion field transforms non-trivial under all these transformations, we end up with a configuration explicitly symmetrised with respect to the full octahedral group.

The tunnelling to the pretzel is somewhat harder to describe in the same terms, but that may not be necessary. We find that there are three – periodic – paths that describe tunnelling possibilities from one tetrahedron to one that is related by a reflection in a plane through the centre of the tetrahedron and parallel to two of the edges (an element of the octahedral and not of the tetrahedral group). Since these have a saddle point at lower energy than the paths through the doughnuts, one expects that they are even more important than those solutions. In essence these paths can be visualised as the edges of a cube, where each closed path is equivalent to one edge.

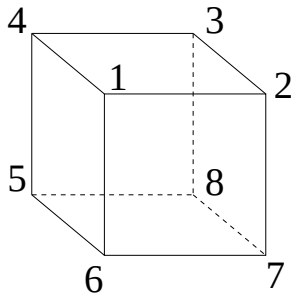

Fig. 16. Labelling of the vertices of the cube. Each corresponds to a different realization of the tetrahedron

If we label the different edges of the cube as in Fig. 16 we can estimate the spectrum using a simple Hückel model, where we only include the nearest-

neighbour interaction diagonalising a simple 8-by-8 Hamiltonian matrix

$$H = \begin{pmatrix} -E_0 & -X & 0 & -X & 0 & -X & 0 & 0 \\ -X & -E_0 & -X & 0 & 0 & 0 & -X & 0 \\ 0 & -X & -E_0 & -X & 0 & 0 & 0 & -X \\ -X & 0 & -X & -E_0 & -X & 0 & 0 & 0 \\ 0 & 0 & 0 & -X & -E_0 & -X & 0 & -X \\ -X & 0 & 0 & 0 & -X & -E_0 & -X & 0 \\ 0 & -X & 0 & 0 & 0 & -X & -E_0 & -X \\ 0 & 0 & -X & 0 & -X & 0 & -X & -E_0 \end{pmatrix}. \tag{45}$$

where we assume all the eight configurations to be orthogonal. E_0 is an estimate for the binding energy within a single well, and X is a mixing matrix element (whose sign will be positive). Since we have to identify even and odd tetrahedra, the only two eigenvectors of this matrix allowed are the symmetric and antisymmetric ones. The eigenvalues are $-E_0 \pm 3X$, and $-E_0 - 3X$ has eigenvector $(1, 1, 1, 1, 1, 1, 1, 1)$.

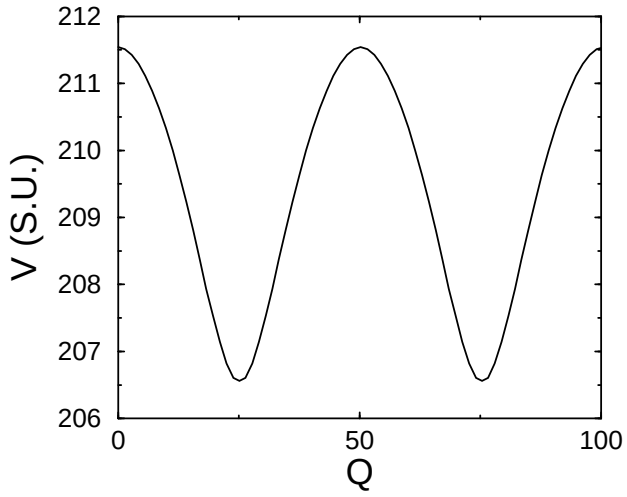

Fig. 17. The potential energy for a full period of motion along the circuit through the pretzels and the tetrahedron.

Since this concerns a lower barrier, it is of greatest relevance to the large amplitude motion. The major issue here is that the harmonic oscillator length parameter for each of the wells is comparable to the length of the circuit for any reasonable value of Skyrme-model parameters. In this case the wave function in the circuit becomes approximately constant, and the energy is the average of the potential along the circuit. Since the contribution of the rotational kinetic

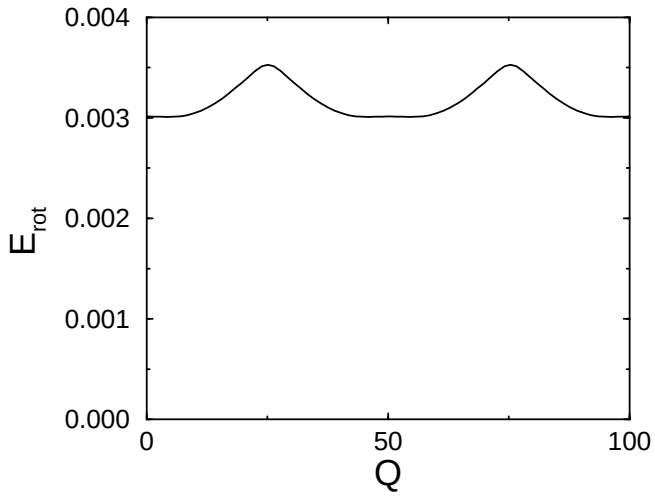

Fig. 18. The expectation value of the rotational energy for a full period of motion along the circuit through the pretzels and the tetrahedron.

energy tends to flatten the potential even more, Fig. 18, this only reinforces this behaviour. If we just naively solve the one-dimensional problem on the circle, we find an energy of $209.5 f_\pi/e + .00319 f_\pi e^3$, a considerable rise in energy. Furthermore, since the pretzel is a lot bigger than the tetrahedron, we find an enhanced value for the r.m.s. radius (by about 10%).

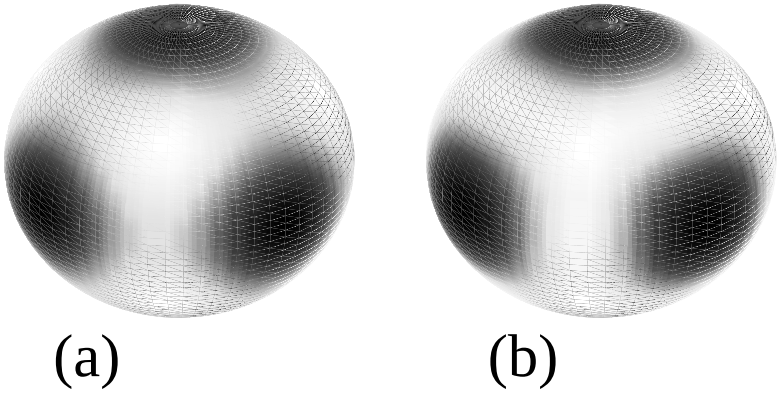

Fig. 19. Two wave functions on the sphere. (a) $x^2y^2 + y^2z^2 + z^2x^2$ and (b) $x^4y^4 + y^4z^4 + z^4x^4 + (x^2y^2 + y^2z^2 + z^2x^2)/2$

For the paths through the doughnut we cannot readily make such an estimate. Even though the harmonic oscillator length parameter is again close to the length of the path, which would imply a similar estimate as above, we cannot ignore the two-dimensional nature of the problem here. If we return to our VSEPR model, the simplest symmetric wave function, that has zeros at the infinities of the potential is $x^2y^2 + y^2z^2 + z^2x^2$ (it is easier to write the wave function in terms of Cartesian tensors than as spherical harmonics). That wave function, as plotted in Fig. 19a, carries non-zero kinetic energy, and a

straightforward calculation shows that

$$\langle K \rangle = \frac{16}{5}\hbar^2. \tag{46}$$

If we make the wave function more strongly centred along the tunnelling paths, as in Fig. 19b, the expectation value of K increases (to $3.63\hbar^2$ for this example). The best possible estimate for the contribution to the ground state energy from the two lowest modes is

$$\Delta E = \frac{1}{R^2}\langle K \rangle + \frac{1}{L}\int (V - E_0)dl + \frac{1}{L}\int E_{\rm rot} dl. \tag{47}$$

Here R is the radius of the sphere associated with a tunnelling path of length L, $L = 2\arctan(\sqrt{\frac{1}{2}})R$. The integral is along one of the tunnelling paths. There are many objections one can make to this approximation (the real collective surface is not exactly a sphere, we ignore the zero-point motion orthogonal to the path, etc.) but we have been unable to come up with a reasonable alternative. We estimate that $\langle L^2 \rangle \approx 3.5\hbar^2$, and calculate the remaining quantities from our results.

Our final model is an independent quantisation of the five lowest non-zero modes, treating the remaining four in harmonic approximation. The potentials for the lowest five modes includes the *difference* of the local harmonic energy and the harmonic energy at the minimum,

$$\tfrac{1}{2}\sum_{i=5}^{9}\hbar\omega(Q) - \tfrac{1}{2}\sum_{i=5}^{9}\hbar\omega(0). \tag{48}$$

The rotational energy is treated in a similar way, i.e., we subtract the result at the minimum. The final result for the ground state energy is

$$E_{gs} = E_{\rm tetrahedron} + \tfrac{1}{2}\sum_{i=5}^{9}\hbar\omega(0) + E_{\rm rot}(0) + \Delta E^{(12)} + 3\Delta E^{(3)}. \tag{49}$$

Here we exhibit that we independent quantise modes three to five, and have an explicit two dimension problem for the lowest two modes. The various quantities in this expression are found to be (obtained in ways discussed above)

$$E_0 = 206.6\frac{f_\pi}{e},$$
$$\tfrac{1}{2}\sum_{i=5}^{9}\hbar\omega(0) = 0.941 f_\pi e,$$

$$
\begin{aligned}
E_{\rm rot}(0) &= 0.00353 f_\pi e^3, \\
\Delta E^{(12)} &= 3.8 f_\pi/e - 0.037 f_\pi e + 0.0028 f_\pi e^3, \\
\Delta E^{(3)} &= 2.9 f_\pi/e - 0.041 f_\pi e - 0.0003 f_\pi e^3.
\end{aligned} \tag{50}
$$

Taking all this together, and subtracting three times the $B = 1$ result, we find

$$
E_{\rm gs} = -1.3 f_\pi/e + 0.781 f_\pi e - 0.007 f_\pi e^3. \tag{51}
$$

If we use our three parameter sets, we find values of 185.5 MeV for ANW, 186.5 MeV for ANW' and 211.6 MeV for R. These values are still high above the threshold, but please note that we have overestimated the effect of the lowest five modes by treating them as independent. Furthermore, some of the higher modes lead to a separated single hedgehog and a doughnut. Our experience from the $B = 2$ case suggests that in such cases the harmonic approximation may be relatively poor, and again leads to an overestimate. We have found a reduction of the energy, however, which is at least promising for a more mature approach to the problem.

8 Conclusions and Outlook

We have shown that our best treatment for the $B = 2$ problem leads to a state close to threshold (a few tens of MeV above or below) for a reasonable choice of parameters. At the moment this uses a enhanced version of the quantisation in the attractive manifold. What is really missing is the Hamiltonian in the full manifold, which is not readily accessible, even though one might consider cross-linking the three channels discussed in our paper, Ref. [1]. Using a different numerical approach to study the modes leading away from the $B = 2$ hedgehog, as done by Waindzoch and Wambach [20], may be another useful tool to get more information. It is unlikely that any of these methods will be able to completely cover the whole collective surface, however.

A more pressing problem is the issue whether we can really construct a decoupled 12-dimensional collective surface. Our results about level crossings in the attractive channel seem to suggest that it may not be possible to do so – or maybe we can, but we need to introduce a monopole geometric phase in our collective Hamiltonian, which should influence the dynamics and the rotational quantum numbers. This is an important issue in the quantisation of the $B = 2$ system.

The $B = 3$ system apparently benefits a lot when the anharmonicities are taking seriously. In the present calculation we have not treated all of them. That is at least partly due to the fact that the JNR instantons are not the

most general ones for this case. The fact that the lowest two modes separate in two bananas instead of three $B = 1$ Skyrmions as the monopole result from Ref. [17] seems to suggest should happen, is probably related to this deficiency.

It is therefore necessary to see whether one can handle the AHDM instanton [21] in calculations of the type performed above. This is not trivial, since the relation between Skyrmion and AHDM data is rather indirect, and may just be too time consuming to implement. We are currently examining the feasibility of this approach. If we can we will be able to better address the anharmonicities for $B = 3$ and probably also see whether large amplitude fluctuations play a rôle for the $B = 4$ system.

Acknowledgements

I thank the Institute for Nuclear Theory at the University of Washington for its hospitality and the Department of Energy for Partial support during the initial stages of this work. I also acknowledge partial support by the Bundesministerium für Forschung und Technologie. I benefited from discussions with N. Manton and C.J. Houghton.

A A detailed analysis of the modes of the tetrahedron.

The instanton field is generated by four poles, arranged in an tetrahedron. All weights are equal. We choose

$$\begin{aligned}
&(\lambda_1, X_1) = (1/4, -R, -R, -R, 0),\\
&(\lambda_2, X_2) = (1/4, -R, R, R, 0),\\
&(\lambda_3, X_3) = (1/4, R, -R, R, 0),\\
&(\lambda_4, X_4) = (1/4, R, R, -R, 0),
\end{aligned} \tag{A.1}$$

where R is a parameter determining the size of the tetrahedron.

Since all continuous symmetries are broken, we find 9 zero modes. In order of increasing frequency the non-zero modes can be interpreted as follows (we concentrate on how the pole positions change. Of course the weights change as well, but it is harder to classify modes that way.) Since we discuss fluctuations here, they have a natural identification as the gradients of a wave function. We shall identify those with the standard molecular orbitals found e.g., in Refs. [18,19]. We shall also apply the standard group representation labels corresponding to these wave functions.

10-11 $\hbar\omega = 0.318 f_\pi e$, irrep=$E$.
The two eigenvectors can be chosen to be

$$\begin{aligned}
&\delta(\lambda_1, X_1) = (0, -1, 1, 0, 0),\\
&\delta(\lambda_2, X_2) = (0, -1, -1, 0, 0),\\
&\delta(\lambda_3, X_3) = (0, 1, -1, 0, 0),\\
&\delta(\lambda_4, X_4) = (0, 1, 1, 0, 0),
\end{aligned} \tag{A.2}$$

and

$$\begin{aligned}
&\delta(\lambda_1, X_1) = (0, -1, -1, 2, 0),\\
&\delta(\lambda_2, X_2) = (0, 1, -1, -2, 0),\\
&\delta(\lambda_3, X_3) = (0, -1, 1, -2, 0),\\
&\delta(\lambda_4, X_4) = (0, 1, 1, 2, 0).
\end{aligned} \tag{A.3}$$

They correspond to the gradient of the standard wave functions $x^2 - y^2$ and $x^2 + y^2 - 2z^2$, respectively. The two modes, both invariant under a rotation around the x-axis, can be interpreted as follows. One mode corresponds to rotating the two lines (12) and (34) relative to one-another around the x-axis. The other correspond to stretching the lines (12) and (34), at the same time moving the lines closer. Both would be expected to go to a planar configuration of poles arranged in a square, the $B = 3$ doughnut.

12-14 $\hbar\omega = 0.332 f_\pi e$, irrep=$T_2$.
One representative of this mode, the one invariant under a 120° rotation about the 111 axis, has the form

$$\begin{aligned}
&\delta(\lambda_1, X_1) = (3\delta\lambda, 1, 1, 1, 0),\\
&\delta(\lambda_2, X_2) = (-\delta\lambda, -1, 0, 0, 0),\\
&\delta(\lambda_3, X_3) = (-\delta\lambda, 0, -1, 0, 0),\\
&\delta(\lambda_4, X_4) = (-\delta\lambda, 0, 0, -1, 0)
\end{aligned} \tag{A.4}$$

The wave function corresponding to the present mode is $-\frac{1}{2}(yz + xz + xy)$, which has led to the T_2 assignment.

In this mode we always keep the three points 2,3,4 in a shrinking equilateral triangle, at the same time moving pole 1 further and further away. This should probably connect to a well separated system consisting of the $B = 2$ doughnut and a single hedgehog.

15-17 $\hbar\omega = 0.469 f_\pi e$, irrep=$T_2$.
One representative of this mode, the one with eigenvalue 1 for a 120° rotation around the 111 axis, has the form

$$\begin{aligned}
&\delta(\lambda_1, X_1) = (-3\delta\lambda, 3, 3, 3, 0),\\
&\delta(\lambda_2, X_2) = (\delta\lambda, -1, 1, 1, 0),\\
&\delta(\lambda_3, X_3) = (\delta\lambda, 1, -1, 1, 0),\\
&\delta(\lambda_4, X_4) = (\delta\lambda, 1, 1, -1, 0)
\end{aligned} \tag{A.5}$$

The change in pole position is up to an overall translation in the $(1,1,1)$ direction the same as found above. The important difference is that the size of $\delta\lambda$ is much larger here (0.274), whereas the value found for the previous modes (.0383) is not incompatible with 0.

Another interpretation is a rescaling of all poles, with a factor $1+\alpha$ for poles 2,3,4 and $1-3\alpha$ for pole 1.

18 $\hbar\omega = 0.483 f_\pi e$, irrep=$A_1$.
This is the breathing mode, as can easily be seen from the mode-vector.

19-21 $\hbar\omega = 0.813 f_\pi e$, irrep=$T_1$.
One representative of this mode, the one with eigenvalue 1 for a 120° rotation around the 111 axis, has the form

$$\begin{aligned}
\delta(\lambda_1, X_1) &= (0,0,0,0,3),\\
\delta(\lambda_2, X_2) &= (0,0,.6278,-.6278,1),\\
\delta(\lambda_3, X_3) &= (0,-.6278,0,.6278,1),\\
\delta(\lambda_4, X_4) &= (0,.6278,-.6278,0,1),\\
\delta(c) &= (1.178,1.178,1.178)
\end{aligned} \tag{A.6}$$

This is the only mode that mixes with iso-spin rotations. The change in the space components is consistent with the irrep T_1 and a wave function $x(y^2-z^2)+y(z^2-x^2)+z(x^2-y^2)$. After a study of the change in baryon number associated with this mode we conclude that it probably corresponds to a twist, where we turn the baryon density in the 234 triangle, keeping the edges fixed at the point 1. At the same time a complicated grooming of the triangle relative to the pole 1 takes place (time-components).

References

[1] N. R. Walet, Nucl. Phys. **A586** (1995), 649 (hep-ph/9410254).

[2] R. A. Leese, N. S. Manton, B. J. Schroers, Nucl. Phys. **B442** (1995) 228 (hep-ph/9502405).

[3] L. Carlson, Phys. Rev. Lett, **66** (1991) 406; Nucl. Phys. **A535** (1991) 479.

[4] R. A. Leese, N. S. Manton, Nucl. Phys. **A572** (1994) 575.

[5] T. S. Walhout, Nucl. Phys. **A547** (1992) 423.

[6] M. F. Atiyah and N. S. Manton, Phys. Lett. B **222** (1989) 438.

[7] M. F. Atiyah and N. S. Manton, Commun. Math. Phys. **153** (1993) 391.

[8] R. Jackiw, C. Nohl, and C. Rebbi, Phys. Rev. D **15** (1977) 1642.

[9] G. Adkins, C. Nappi, and E. Witten, Nucl. Phys. **B228** (1983) 552.

[10] H. Goldstein, *Classical Mechanics* (Addison Wesley, Reading, 1981).

[11] P. Ring and P. Schuck, *The Nuclear Many-Body Problem*, (Springer, Berlin, 1980).

[12] R. J. Gillespie and I. Hargittai, *The VSEPR Model of Molecular Geometry* (Allyn and Bacon, 1991).

[13] B. Moussalam, Ann. Phys. (NY) **225** (1993) 264.

[14] G. Pöschl and E. Teller, Z. Phys. **83** (1933) 143; N. Rosen and P. Morse, Phys. Rev. **42** (1932) 210.

[15] J. N. Ginocchio, Ann. Phys. (NY) **152** (1984) 203

[16] N. R. Walet, Phys. Rev. **C48** (1993) 222 (nucl-th/9306001).

[17] C. J. Houghton and P. M. Sutcliffe, Monopole scattering with a twist, preprint DAMTP 95-28, Nucl. Phys **B** in press (hep-th/9601148).

[18] J. Q. Chen, *Group Representation Theory for Physicists* (World Scientific, Singapore, 1989) pp. 386-394.

[19] M. Tinkham, *Group Theory and Quantum Mechanics* (McGraw-Hill, New York, 1964) pp. 323-330.

[20] T. Waindzoch and J. Wambach, "Stability of the B=2 hedgehog in the Skyrme model", Report KFA-IKP(TH)-1995-22 (hep-ph/9509421).

[21] M. F. Atiyah, N. J. Hitchin, V. G. Drinfeld, and Yu. I. Manin, Phys. Lett. **65A** (1978) 185.